Using Singularities of Parallel Manipulators for Enhancing the Rigid-body Replacement Design Method of Compliant Mechanisms

Lennart Rubbert, Stéphane Caro, Jacques Gangloff, Pierre Renaud

Using Singularities of Parallel Manipulators to Enhance the Rigid-body Replacement Design Method of Compliant Mechanisms

L. Rubbert*, S. Caro, J. Gangloff and P. Renaud
Instant-Lab, ICube, IRCCyN
Ecole Polytechnique Federale of Lausanne - University of Strasbourg -
INSA of Strasbourg - Ecole Centrale Nantes, CNRS
Switzerland, France
Email: lennart.rubbert@epfl.ch
stephane.caro@irccyn.ec-nantes.fr
jacques.gangloff@unistra.fr
pierre.renaud@insa-strasbourg.fr

The rigid-body replacement method is often used when designing a compliant mechanism. The stiffness of the compliant mechanism, one of its main properties, is then highly dependent on the initial choice of a rigid-body architecture. In this paper, we propose to enhance the efficiency of the synthesis method by focusing on the architecture selection. This selection is done by considering the required mobilities and parallel manipulators in singularity to achieve them. Kinematic singularities of parallel structures are indeed advantageously used to propose compliant mechanisms with interesting stiffness properties. The approach is first illustrated by an example, the design of a one degree of freedom compliant architecture. Then the method is used to design a medical device where a compliant mechanism with three degrees of freedom is needed. The interest of the approach is outlined after application of the method.

1 Introduction

Compliant mechanisms are monolithic structures taking advantage of elasticity to produce movements. The absence of backlash and friction allows the production of very accurate movements making them suitable for medical devices [1–3], micropositioning [4, 5] and space applications [6]. One challenge is to design compliant mechanisms with multiple degrees of freedom that have adequate stiffness performances, *i.e.* that demonstrate low stiffnesses along the desired degrees of freedom (DOF), high stiffnesses in the other directions, and that fulfill other design criteria such as compactness. There are different ways to design compliant mechanisms. The most common synthesis approaches, described in [7], are the kinematic-based approaches, the building blocks approaches and the structural optimization-based approaches. Among the kinematic-based approaches, the FACT method does not require knowledge of existing rigid-body mechanisms, the synthesis being performed using screw theory [8, 9]. The rigid-body replacement approach is very interesting since it takes advantage of the large number of existing rigid-body mechanisms and their modeling tools [10]. With this approach, a rigid-body mechanism is first designed, or selected in the literature, then converted into a compliant mechanism, followed by pseudo-rigid body modeling [11] and optimization. Complex compliant mechanisms with multiple DOF can thus be obtained [5, 12–14].

The design or selection of the rigid-body mechanism architecture, which will be used for the compliant mechanism synthesis, is critical. For identical mobilities, the mechanism architecture can be, for instance, serial or parallel. For a mechanism composed of a serial linkage, a direct conversion into a compliant structure may lead to insufficient stiffness performances, whatever the geometry of the flexure joints is. In such a situation, it is interesting to provide the designer with alternative solutions. Olsen *et al.* proposed a classification scheme to identify subgroups in a mechanism which can be independently converted into compliant elements [10, 15]. The main idea is that some subchains from an initial architecture can be efficiently replaced by alternative architectures to improve the final performances of the compliant mechanism. The use of parallel architectures has been proposed for this purpose because of their interesting intrinsic stiffness properties. Selecting or proposing a parallel mechanism is however a delicate task. First, even though many parallel architectures exist [16], the choice of a parallel mechanism with particular mobilities is generally not obvious. Second, each parallel mechanism has its own workspace and its kinematic properties are strongly dependent on the mechanism configuration [17]. Therefore, selecting a parallel mechanism also requires an expertise in the definition of the configuration used for the compliant mechanism.

One well-known feature of parallel mechanisms is the existence of so-called singular configurations. In those configurations, the parallel mechanism locally exhibits specific mobilities. Since compliant mechanisms usually work around a given position, it seems interesting to start their design with the architectures obtained from parallel mechanisms in singularity, for three reasons. First, the designer only has to focus on the selection of a parallel architecture with adequate singular configurations, instead of having to select a parallel mechanism and afterward a configuration. Second, the designer can benefit from the knowledge of singularity analysis for many parallel manipulators [16, 18]. It is then easy to obtain mechanisms that can achieve particular mobilities with parallel architectures for the sake of stiffness. Third, many spatial parallel manipulators reach a singular configuration in planar configurations. Planar configurations are of particular interest for the design of compliant mechanisms since their manufacturing is usually largely simplified [19, 20].

In this paper, the singularity analysis of parallel manipulators is considered in the type-synthesis of compliant mechanisms based on the rigid-body replacement approach. Therefore, the singularities of parallel manipulators, that are generally avoided, are here at the center of a design approach.

In Section 2, we detail how a parallel manipulator and its singularities can be used to design a parallel architecture that can be integrated later in a compliant mechanism. The approach is illustrated with the design of a simple 1-DOF compliant mechanism. The design of an active cardiac stabilizer, a medical device, is performed by using rigid-body replacement method in Section 3. The use of the proposed approach is outlined, with the introduction of an original parallel architecture in the compliant device. The performance of the mechanism is evaluated and its interest is discussed before drawing a conclusion on the relevance of the approach.

2 The Design Approach

The proposed approach for rigid-body mechanism selection is intrinsically related to the singularities of parallel manipulators. They are first briefly outlined. Then details are given on how mechanism selection can be achieved by using them.

2.1 Singularities of Parallel Manipulators

For a given parallel manipulator, $\mathbf{q}_a$ and $\mathbf{q}_p$ denote the actuated joint angle vector and the passive joint angle vector, respectively. The full twist $\mathbf{T}$ describes the velocities along the 6-DOF of the end-effector. It can be divided into $\mathbf{T}_n$, the velocities of the n-DOF of the end-effector of the manipulator, and $\mathbf{T}_{\bar{n}}$, the complementary velocities which should be zero in the normal case. The relationship between the input velocities of the actuators $\dot{\mathbf{q}}_\mathbf{a}$, the passive joint velocities $\dot{\mathbf{q}}_\mathbf{p}$ and the full twist of the end-effector $\mathbf{T}$ can be written as [16, 21]:

$$\mathbf{A}\dot{\mathbf{q}}_\mathbf{a} + \mathbf{B}\mathbf{T} + \mathbf{C}\dot{\mathbf{q}}_\mathbf{p} = 0 \tag{1}$$

This equation can be rewritten as:

$$L(\dot{\mathbf{q}}_\mathbf{a}, \dot{\mathbf{q}}_\mathbf{p}, \mathbf{T})^T = 0 \tag{2}$$

where L is a $N \times (N+n)$ matrix, N being the number of equations and $N+n$ the number of unknowns.

If the end-effector does not move while the actuators have non-zero velocities, the manipulator is in a serial singularity, or redundant input singularity (Type 1 [22]). Therefore it can be said that the end-effector loses one or more DOF. Inversely, if the end-effector of the manipulator can move locally even if the actuators are locked and $\|\mathbf{T}_\mathbf{n}\| \neq 0$ the manipulator is in a parallel singularity, or redundant output singularity (Type 2 [22]). It can be said that the end-effector gains one or more DOF. The manipulator is in a Type 3 singularity if the manipulator reaches both serial and parallel singularities. In case of a parallel singularity, if $\|\mathbf{T}_\mathbf{n}\| = 0$ and $\|\mathbf{T}_{\bar{\mathbf{n}}}\| \neq 0$, the manipulator reaches a constraint singularity that includes the case of architectural singularity where self-motions occur and the end-effector can move with finite amplitude [16, 23]. If the actuators are locked, $\|\mathbf{T}\| = 0$ and the passive joints can move, the manipulator is in a redundant passive motion singularity.

Here, the redundant output singularities where the end-effector moves while the actuators are locked are interesting for the design of compliant mechanisms. As a matter of fact, as a compliant mechanism only works around a given configuration, the motions of the moving platform can be used to produce the required displacements. At the same time, the actuated joints can be suppressed as they are considered locked, which simplifies the architecture of the compliant mechanism.

It is noteworthy that Type 2 singularities have already been considered for simple mechanisms, for instance in the case of orthoplanar mechanisms [24] or the development of 1-DOF structures such as torque sensors [25, 26], but have never been applied in a more generic way to compliant mechanisms.

2.2 Principle of the Design Approach

The approach to select a rigid-body mechanism from parallel mechanisms in a singular configuration is introduced with the example of the design of a 1-DOF compliant mechanism equivalent to a revolute joint. The approach is broken down into four steps.

Step 1 - Selection of a mechanism: First, a parallel manipulator needs to be selected or identified. It needs to exhibit in singularity at least the desired mobilities of the compliant linkage. Here, the 3-PRR planar parallel manipulator illustrated in Figure 1a is chosen. The singularity analysis of this manipulator was performed in [27]. The manipulator has a planar architecture and is composed of three identical

limbs and has three degrees of freedom. Each limb contains a prismatic actuated joint and two passive revolute joints. The 3-PRR can reach some parallel singularities and the gained motions are instantaneous rotations about an axis normal to the plane of motion.

Step 2 - Singularity analysis: For a given architecture, the nature of the displacements in singularity depends on the actuated joints, *i.e.* the actuation mode. For parallel singularities, the end-effector motion is obtained while the actuated joints are locked. The choice of these actuated joints is crucial for the design of the compliant structure since this latter is obtained by their suppression. Consequently, Step 2 consists in analyzing all possible actuation modes for the selected architecture, in order to identify the one that most simplifies the subsequent compliant structure.

In the case of the 3-PRR architectures, their singular configurations have been analyzed with the screw theory [27]. Considering symmetrical actuation modes, *i.e.*, the same joint in each leg is actuated, a singular configuration of Type 2 exists for the three possible actuation modes. Considering the 3-PRR parallel manipulator, the singular configuration occurs when the lines associated with the distal links intersect at a single point as illustrated in Figure 1b. Considering the 3-PRR parallel manipulator and the 3-PRR parallel manipulator, their singular configurations of Type 3 occur when the lines associated with the distal links intersect at one point and are normal to the axis of their prismatic joint as illustrated in Figure 1c and Figure 1d.

Step 3 - Actuation mode selection: If different actuation modes allow the manipulator in singularity to have the desired mobilities, the one which simplifies the most the compliant mechanism architecture and its manufacturing is selected. It is noteworthy that revolute joints are the simplest and easiest-to-manufacture joints [28]. A prismatic joint is more complex to manufacture as it requires at least two leaf-spring joints or four notch joints [29]. A compliant mechanism only composed of compliant revolute joints may therefore be preferred. If a parallel manipulator is composed of joints of the same kind, *i.e.* it is only composed of revolute joints or prismatic joints, the designer has to choose the actuation mode that mostly simplifies the conversion to a compliant mechanism: decision criteria will be based on the manufacturing process, the global arrangement with respect to space requirements.

Here, the architecture illustrated in Figure 1e, obtained from the first actuation mode after suppression of the prismatic joints, has only revolute joints and is therefore preferred.

Step 4 - Design of the compliant mechanism: The simplified kinematic architecture can now be converted to a compliant mechanism by replacing each joint by a notch joint. Here, the 3-RR architecture of the final compliant mechanism is illustrated in Figure 1f.

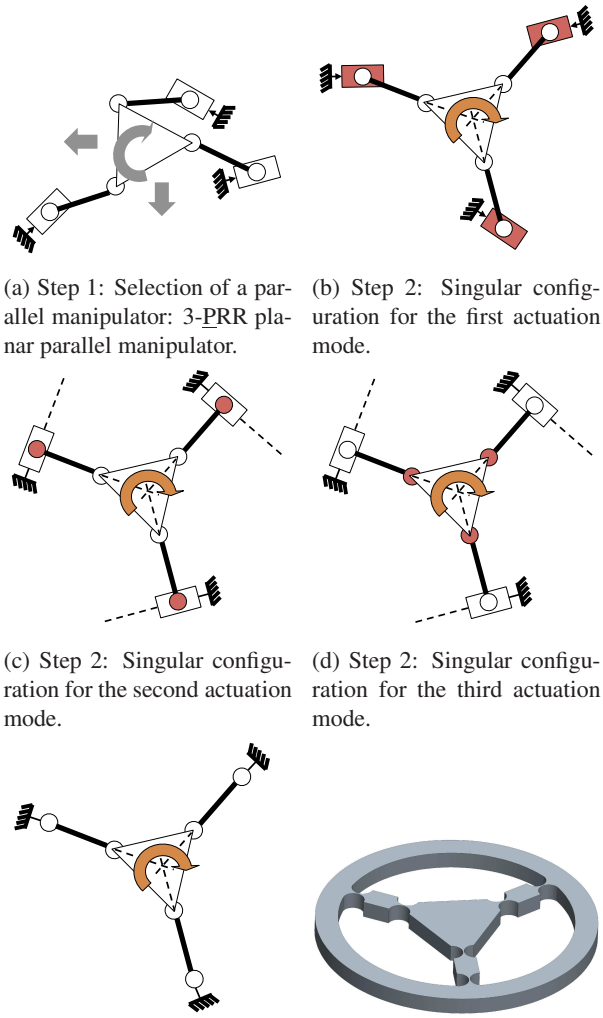

(a) Step 1: Selection of a parallel manipulator: 3-PRR planar parallel manipulator.

(b) Step 2: Singular configuration for the first actuation mode.

(c) Step 2: Singular configuration for the second actuation mode.

(d) Step 2: Singular configuration for the third actuation mode.

(e) Step 3: Selection of the most suitable actuation mode.

(f) Step 4: Design of the compliant mechanism.

Fig. 1: Principle of the design approach based on singularity analysis of parallel manipulators. Colored joints represent the actuated joints considered locked, big arrows represent the possible instantaneous motions of the end-effector.

3 Design of a Compliant Mechanism for an Active Cardiac Stabilizer

The design approach which was introduced in the previous section is now applied in the context of a medical device design. The aim of this section is first to show the interest of the proposed approach during the design of a compliant device, and second to show its potential efficiency, with the introduction of a non-trivial 3-DOF mechanism.

3.1 The Design Problem

Coronary artery bypass grafting is a common procedure in cardiac surgery. It usually requires the use of a heart-lung machine to ease the task, with possible side-effects for the patient. A solution is to perform grafting procedures on the surface of a beating heart, its surface being locally immobilized with a so-called active cardiac stabilizer [30]. It is

an active compliant mechanism controlled by vision that detects any heart displacement and suppresses it by modifying the position of a shaft applied on the heart. It can be compared to an active compensation device cancelling in real time the influence of the heart contraction. The most recent device, *Cardiolock 2*, is illustrated in Figure 2. It provides the 2 DOF needed for the compensation task [31]. The actuation is performed with piezoelectric stacks because of their accuracy and large bandwidth. In presence of the 5 N cardiac forces, the stabilizer exhibits displacements at its tip due to its own flexibilities and the lack of stiffness of its mounting system [12]. Consequently, the device must be able to compensate for these displacements at the shaft tip in the two directions perpendicular to the shaft axis. Piezoelectric stacks have very limited stroke, so that an amplification mechanism is necessary in order to obtain the required displacements [31].

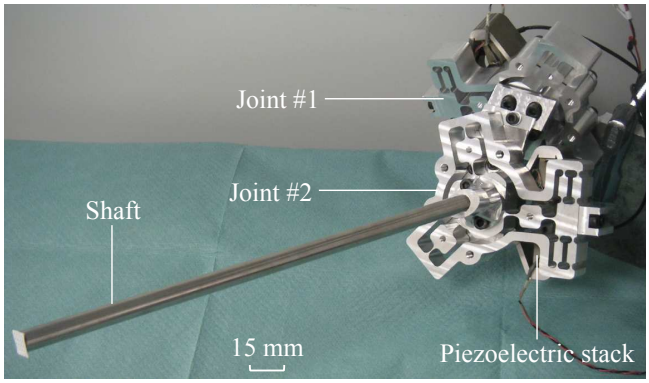

Fig. 2: The *Cardiolock II* [31].

At this point, the compactness of this device needs to be increased to meet the requirements of an operation room while maintaining the same level of performances. As a consequence, we consider as a new architecture the kinematic scheme represented in Figure 3. The stabilizer is then composed of two prismatic joints in P_1 to control the orientation of the shaft with respect to the base, thanks to a spherical joint located in O_2. The variation of the shaft orientation and the distance between O_1 and O_2 require the interconnection of O_1 andO_2 by a universal joint and a prismatic joint (Fig. 3).

The two serially-connected prismatic joints in the plane P_1 can be easily designed as a parallel planar mechanism, for instance with the solutions presented in [32–34], in order to minimize the compliance of the mechanism that can lower the achievable shaft displacements.

The design of a compliant spherical joint by means of a planar parallel mechanism of 3-RRR type has been previously developed in [35]. This mechanism can be placed in O_2. With two planar architectures, one in P_1 and one in P_2 (Fig. 3), it becomes easy to minimize the distance a between the two planes, and finally amplify the displacements given by the piezoelectric stacks in P_1 thanks to the ratio between

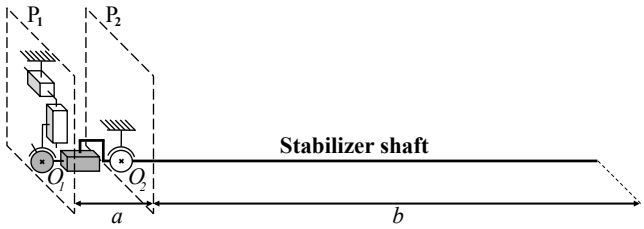

Fig. 3: The new considered architecture for the active stabilizer.

a and b, the length of the shaft. Compactness should also be improved by stacking two planar compliant structures together.

A serial subgroup with RRP mobilities, *i.e.* the DOF of a universal joint (RR) serially connected to a prismatic joint(P), connects the spherical joint and the end of the shaft in O_1. At this point, it needs to be designed. Piezoelectric stacks will deliver high forces to counterbalance the cardiac forces exerted on the shaft tip. The subgroup will therefore be subjected to high loads. Converting the RRP chain in three serially connected equivalent compliant joints may lead to a compliant structure with limited stiffness, that will exhibit significant deflections. Therefore, this section deals with the design of a planar compliant mechanism with RRP mobilities.

3.2 Step 1: Selection of a Mechanism: the 3-US Parallel Manipulator

An interesting parallel mechanism is the 3-DOF 3-US mechanism, considered for lamina emergent mechanisms and for foldable mechanisms [36, 37], illustrated in Figure 6.

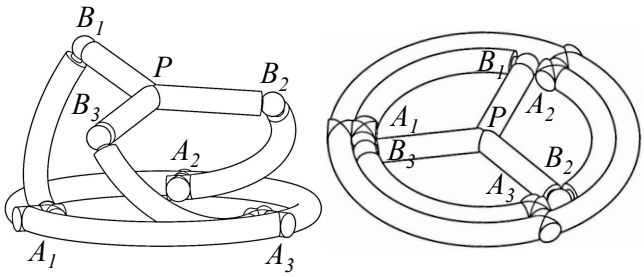

Fig. 4: 3-US parallel manipulator and its planar configuration.

The architecture of the 3-US mechanism is interesting since it has three identical legs only composed of a universal joint in A_i and a spherical joint in B_i that can be broken down into five revolute joints, which are easy to manufacture.

Here, the planar configuration is interesting as the possible motions of the end-effector are translations normal to the plane of the mechanism (Fig. 5a) and rotations around

the axes in the plane of the mechanism (Fig. 5b and Fig. 5b). So, in the planar configuration, the end-effector of the 3-US mechanism has precisely the RRP mobilities.

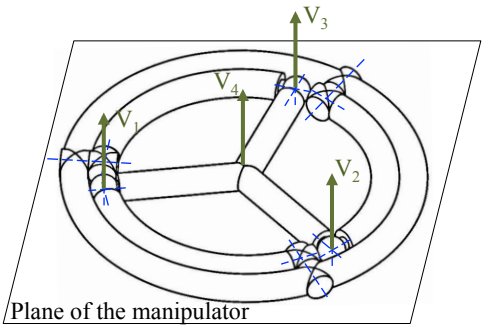

(a) Translation velocity vector field.

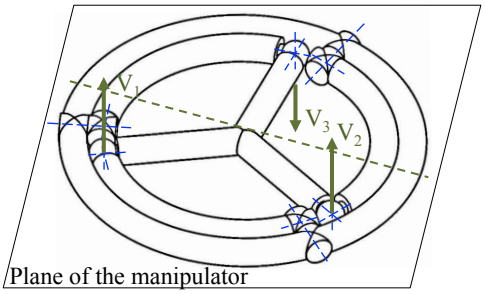

(b) First rotation velocity vector field.

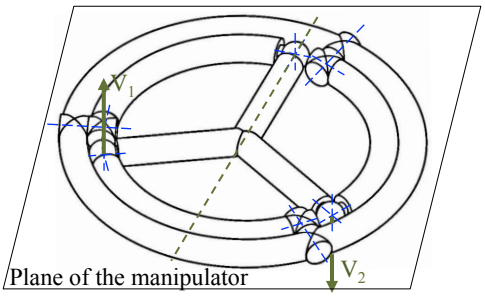

(c) Second rotation velocity vector field.

Fig. 5: Instantaneous motions of the 3-US manipulator in the planar configuration.

Moreover, in the planar configuration, at least one Type 2 singular configuration can be identified. In fact, if the first or the second revolute joints of the universal joints are locked, it is not possible to counterbalance the normal forces applied to the end-effector. In this case, the end-effector exhibits instantaneous motions corresponding to the desired RRP mobilities.

As for the design of the 1-DOF compliant mechanism illustrated in the previous section, the architecture of the 3-US may be simplified in a 3-RS mechanism. But another simplified architecture could be obtained in the planar configuration with another actuation mode that would finally ease the design and the manufacturing of the compliant mechanism. We therefore perform the singularity analysis of the 3-US in the planar configuration for the different possible actuation modes.

3.3 Step 2: Singularity Analysis of the 3-US Parallel Manipulator for Different Actuation Modes

Each leg of the 3-US parallel mechanism is composed of a universal joint and a spherical joint. The universal joint is similar to two revolute joints with perpendicular and intersecting axes. The spherical joint can be broken down into three revolute joints with perpendicular and intersecting axes as shown in Figure 6.

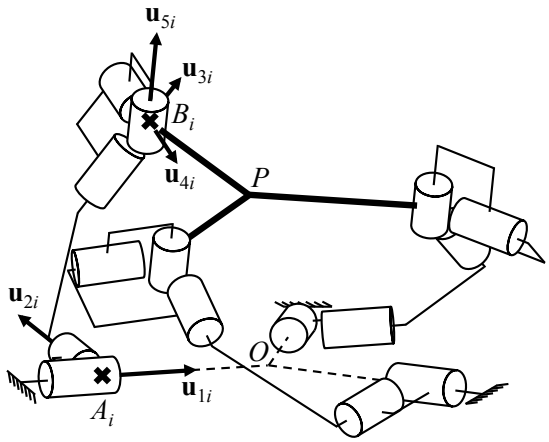

Fig. 6: 3-US manipulator broken down into rotational joints.

Hence, there are $\binom{15}{3} = 455$ possible actuation modes. Among these 455 modes, 5 of them are symmetric, *i.e.* the same rotational joint on each leg is actuated. If we consider that the manipulator has similar legs, there are also 150 unique asymmetric actuation modes. Among these 155 possible unique actuation modes there may be many singular configurations which could lead to different compliant mechanism architectures.

Analyzing the five symmetric actuation modes of the 3-US parallel manipulator is indeed sufficient to analyze the 155 possible unique actuation modes. This will be shown later in the paper, after detailing the singularity analysis of the symmetric actuation modes.

A direct analysis of the singularities of the extended forward Jacobian matrix involves the calculation of its determinant which may be a difficult task even with symbolic computation softwares [16]. Here, the singularities are analyzed with the screw theory [38], which allows us to obtain the global wrench system of the manipulator. In fact, the degeneration of the global wrench system of a parallel manipulator is directly related to the degeneration of its extended forward kinematic Jacobian matrix. The singularity analysis of the 3-US manipulator is therefore performed through the analysis of its global wrench system degeneration. In [39] the singularity analysis of the mechanism was

performed in the whole workspace for the five symmetric actuation modes. Screw theory and Grassmann-Cayley algebra were then used. Here, we perform the singularity analysis for all possible actuation modes of the 3-US manipulator but only in the planar configuration. In this situation, the use of the screw theory is sufficient.

The global wrench system of the 3-US is spanned by the constraint wrench system and its actuation wrench system. The constraint wrench system describes how the end-effector is constrained by the leg of the manipulator and the actuation wrench system describes how the actuators act on the end-effector. Therefore, in a non-singular pose, the global wrench system describes how the end-effector is mechanically fully constrained. If the global wrench system degenerates, the end-effector is no more constrained and the manipulator reaches a parallel singularity.

3.3.1 Twist system of the 3-US

A *twist* is a screw representing the instantaneous motion of a rigid body. An infinite-pitch twist ε_∞ represents a pure translation, whereas a zero-pitch twist ε_0 represents a pure rotation. As the 3-US can be represented using only revolute joints, the twist system T^i associated with the i-th leg of the 3-US is spanned by five zero-pitch twists defined as [38]:

$$\hat{\varepsilon}^i_{01} = \begin{bmatrix} \mathbf{u}_{1i} \\ \mathbf{a}_i \times \mathbf{u}_{1i} \end{bmatrix}, \hat{\varepsilon}^i_{02} = \begin{bmatrix} \mathbf{u}_{2i} \\ \mathbf{a}_i \times \mathbf{u}_{2i} \end{bmatrix} \hat{\varepsilon}^i_{03} = \begin{bmatrix} \mathbf{u}_{3i} \\ \mathbf{b}_i \times \mathbf{u}_{3i} \end{bmatrix}$$
$$\hat{\varepsilon}^i_{04} = \begin{bmatrix} \mathbf{u}_{4i} \\ \mathbf{b}_i \times \mathbf{u}_{4i} \end{bmatrix}, \hat{\varepsilon}^i_{05} = \begin{bmatrix} \mathbf{u}_{5i} \\ \mathbf{b}_i \times \mathbf{u}_{5i} \end{bmatrix}, \quad i = 1,2,3 \qquad (3)$$

$\mathbf{u}_{1i}$ and $\mathbf{u}_{2i}$ are the unit vectors of the first and second revolute joint axes of the universal joint of the i-th leg. $\mathbf{u}_{3i}$, $\mathbf{u}_{4i}$ and $\mathbf{u}_{5i}$ are the unit vectors of the revolute joints associated with the spherical joint of the i-th leg. $\mathbf{a}_i$ and $\mathbf{b}_i$ are the Cartesian coordinate vectors of points A_i and B_i shown in Figure 6. The twist system T of the 3-US is the intersection of T^1, T^2 and T^3, namely,

$$\mathrm{T}_{3US} = \bigcap_{i=1}^{3} \mathrm{T}^i \qquad (4)$$

3.3.2 Constraint wrench system

A *wrench* is a screw representing a system of forces and moments acting on a rigid body. The constraint wrench system describes how the legs constrain the end-effector of the 3-US parallel manipulator. Hence, for each leg, the constraint wrench associated to the leg must be reciprocal to the twist system T^i of the leg. In a non-singular configuration, the constraint wrench system W^c of the 3-US is a three-system spanned by the following three pure forces (Fig. 7):

$$\hat{\mathscr{F}}^c_i = \begin{bmatrix} \mathbf{n}_i \\ \mathbf{b}_i \times \mathbf{n}_i \end{bmatrix}, \quad i = 1,2,3 \qquad (5)$$

$\mathbf{n}_i$ being the unit vector of $\overrightarrow{A_iB_i}$.

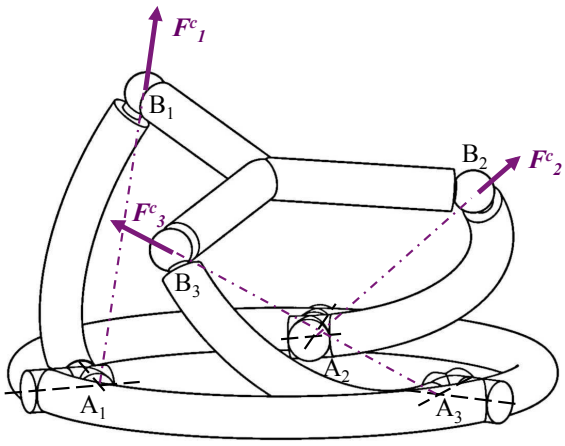

Fig. 7: Constraint forces applied by the legs to the moving-platform.

3.3.3 Actuation wrench system

The actuation wrench system W^a of the 3-US manipulator depends on its actuation scheme and describes how the actuators act on the end-effector. Hence, for each leg, the actuation wrench should be reciprocal to the twists in the leg, except for the twist associated with the actuated joint. Moreover, it should lie in the constraint wrench system W^c. In case the first revolute joint of each leg is actuated, W^a is spanned by the following three pure forces, called actuation forces (Fig. 8):

$$\hat{\mathscr{F}}^a_{1i} = \begin{bmatrix} \mathbf{u}_{2i} \\ \mathbf{b}_i \times \mathbf{u}_{2i} \end{bmatrix}, \quad i = 1,2,3 \qquad (6)$$

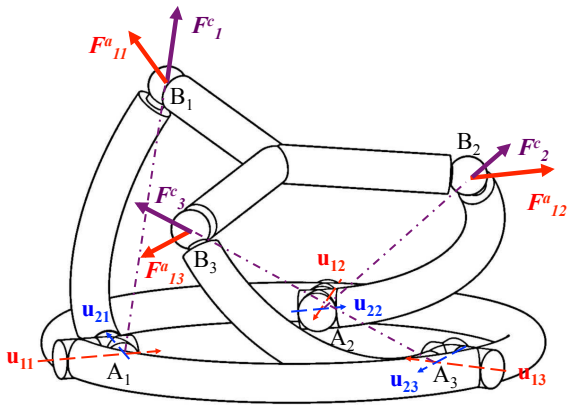

Fig. 8: Constraint and actuation wrench system of the 3-US parallel manipulator for the first actuation mode.

In case the second revolute joint of each leg is actuated,

$\mathbb{W}^a$ is spanned by the following three pure forces:

$$\hat{\mathscr{F}}^a_{2i} = \begin{bmatrix} \mathbf{u}_{1i} \\ \mathbf{b}_i \times \mathbf{u}_{1i} \end{bmatrix}, \quad i = 1,2,3 \tag{7}$$

In case the j-th revolute joint of each leg is actuated, $j = 3,4,5$, $\mathbb{W}^a$ is spanned by the following three pure forces:

$$\hat{\mathscr{F}}^a_{ji} = \begin{bmatrix} \mathbf{v}_{ji} \\ \mathbf{c}_{ji} \times \mathbf{v}_{ji} \end{bmatrix}, \quad i = 1,2,3 \tag{8}$$

$\mathbf{v}_{ji}$ being the unit vector of the intersection line $\mathscr{L}_{ji}$ of planes $\mathscr{P}_{1i}$ and $\mathscr{P}_{ji}$. $\mathbf{c}_{ji}$ is the Cartesian coordinate vector of any point C_{ji} on line $\mathscr{L}_{ji}$. $\mathscr{P}_{1i}$ is spanned by vectors $\mathbf{u}_{1i}$ and $\mathbf{u}_{2i}$ and passes through point A_i. $\mathscr{P}_{3i}$ is spanned by vectors $\mathbf{u}_{4i}$ and $\mathbf{u}_{5i}$ and passes through point B_i. $\mathscr{P}_{4i}$ is spanned by vectors $\mathbf{u}_{3i}$ and $\mathbf{u}_{5i}$ and passes through point B_i. $\mathscr{P}_{5i}$ is spanned by vectors $\mathbf{u}_{3i}$ and $\mathbf{u}_{4i}$ and passes through point B_i (Fig. 9 for the fourth actuation mode).

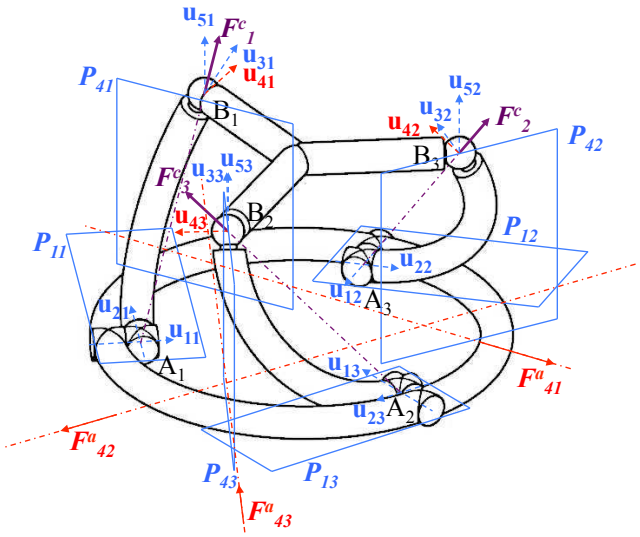

Fig. 9: Constraint and actuation forces of the 3-US parallel manipulator for the fourth actuation mode.

3.3.4 Global wrench system

Let k be the number of the actuated joint in each leg for the k-th actuation mode of the mechanism, $k = 1,\ldots,5$. As a result, the global wrench system $\mathbb{W}^k_{3US}$ of the 3-US associated with its k-th actuation scheme is spanned by $\mathbb{W}^a$ and $\mathbb{W}^c$, namely,

$$\mathbb{W}^k_{3US} = span(\hat{\mathscr{F}}^c_1, \hat{\mathscr{F}}^c_2, \hat{\mathscr{F}}^c_3, \hat{\mathscr{F}}^a_{k1}, \hat{\mathscr{F}}^a_{k2}, \hat{\mathscr{F}}^a_{k3}), \quad k = 1,\ldots,5 \tag{9}$$

3.3.5 Instantaneous gained motions

For the manipulator in the planar configuration and for the five symmetrical actuation modes, the three actuation forces are in the plane of the manipulator (Fig. 10a). It means that the actuation wrench system degenerates and the 3-US manipulator reaches a parallel singularity in such a configuration. As the three actuation forces are coplanar, the actuators are not able to counterbalance the forces normal to the end-effector and the moments around the axes in the plane of the manipulator.

In section 3.3.3 we have seen that actuating any of the five revolute joints of a leg produces an actuation force in the plane of the planar configuration. In other words, there is no actuation mode that produces non-coplanar actuation forces. It means that for any of the 150 asymmetrical possible actuation modes, the actuation wrench system will always be composed of coplanar pure forces in the planar configuration of the 3-US manipulator. As a consequence, the planar configuration of the 3-US parallel manipulator is, for the 155 possible actuation modes, a singular configuration of Type 2 where the end-effector exhibits the desired instantaneous RRP mobilities. 155 unique architectures can thus be considered to design a compliant structure with adequate mobilities. Design and manufacturing considerations are used to make a selection.

3.4 Step 3: Selection of an actuation mode

A first remark is that the design of a spherical compliant joint is complex. In fact, two design options can be considered. One solution consists in designing a single revolute notch [40]. With this solution, the ratio between the translational and the rotational stiffnesses along the revolution axis of this joint can be low. Thus, the kinematic behavior would be different of that of a spherical joint. Moreover, the small cross-section can lead to high stresses. A second solution consists in designing a spherical compliant joint with three compliant revolute joints. Stiffness properties are improved, but since we would like to have a device composed of two planar mechanisms, the joint needs to be machined in a plate. Manufacturing three compliant revolute joints with orthogonal and intersecting axes as proposed by [40] is then complex. It is more interesting to choose an actuation mode which allows to suppress one revolute joint that composes the spherical joints and therefore to have a compliant mechanism only composed of universal joints.

In order to machine this planar structure, it is more convenient to machine flexure joints with revolute joint axes in the plane. Hence, it seems easier to consider the fifth symmetric actuation mode ($\mathbf{u}_{5i}$, Fig. 6), which suppresses the three revolute axes normal to the base and moving platform in the planar configuration of the 3-US manipulator. As a result, the 3-US architecture becomes a 3-UU architecture as illustrated in Figure 11.

To the best of our knowledge, such an architecture has never been considered to obtain this type of mobilities. Without the proposed approach, it would have been very difficult to identify this structure for the design of the active stabilizer.

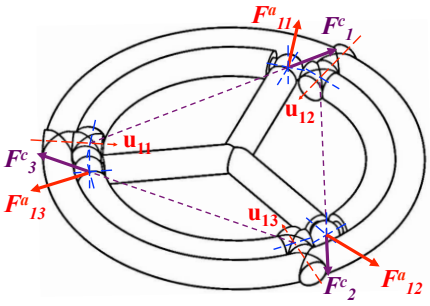

(a) First actuation mode.

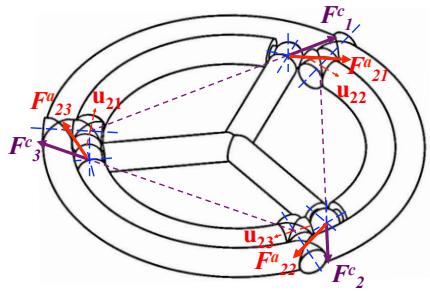

(b) Second actuation mode.

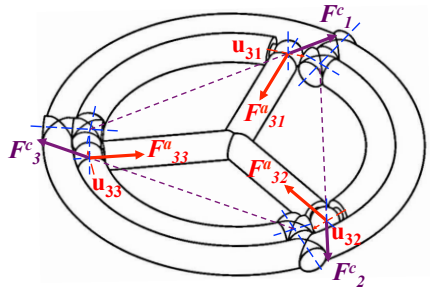

(c) Third actuation mode.

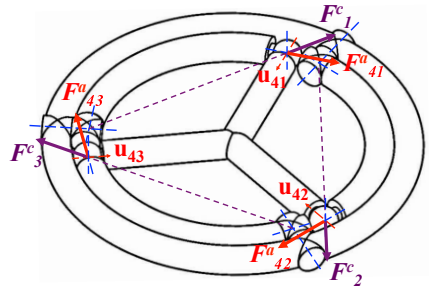

(d) Fourth actuation mode.

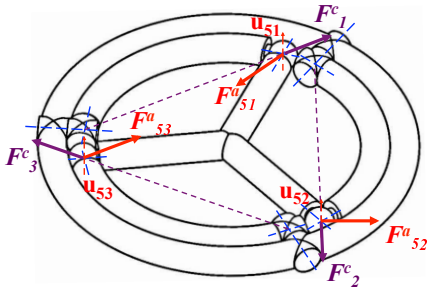

(e) Fith actuation mode.

Fig. 10: Constraint and actuation forces of the 3-US parallel manipulator for the five actuation modes.

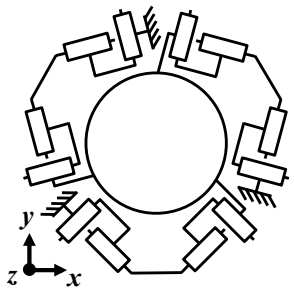

Fig. 11: 3-UU planar mechanism with RRP mobilities.

3.5 Step 4: Design of the compliant mechanism

The 3-UU compliant mechanism is only composed of universal joints. Interesting designs of compliant universal joints have been proposed in [40] and [41], but they can not be manufactured in a planar structure or requires an assembly.

We therefore propose for the design of the compliant universal joints to manufacture two compliant revolute joints in the plane with intersecting axes in A_i or B_i depending on the considered universal joint. The 3-UU compliant mechanism is then designed by replacing each revolute joint by a circular flexure hinge. A computer-aided design (CAD) of the compliant 3-UU mechanism is shown in Figure 12.

Fig. 12: CAD view of the 3-UU compliant mechanism.

The dimensional synthesis of the obtained compliant mechanism is performed by considering the other elements that compose the active stabilizer, *i.e.* the two prismatic joints and the spherical joint.

The length of the stabilizer shaft $b = 250$ mm is constrained by the medical context. The only way to modify the amplification ratio of the device is therefore to modify the distance a between planes P_1 and P_2. The distance a can not exceed 12 mm (Fig. 3) to get sufficient shaft displacements. In this situation, static analysis shows that the PZT stacks deliver forces above 100 N in O_1.

For a first dimensional synthesis of the 3-UU mechanism, a trial-and-error design is performed using finite element analysis (FEA). To limit the number of possibilities, we only tuned two design parameters: the radius and the thickness of the circular notches. As a matter of fact, the notch thicknesses mainly influence the global stiffness of the compliant structure and the circular notch radius mainly in-

fluences the level of the stress concentration. The goal is then to find a good compromise between output displacement amplitude of the whole mechanism and the maximal stress level. Finally, the thickness of the 3-UU mechanism and the outer radius of its legs have been chosen equal to 5 mm and 35 mm, respectively. The compliant joints have a thickness equal to 0.2 mm, a width equal to 15 mm and the radius of the circular notches is equal to 2 mm.

3.6 Performances of the compliant mechanism

With the considered design, PZT stacks should apply forces in the order of 300 N on the planar 3-UU compliant mechanism in order to counterbalance the cardiac forces during the stabilization task. Stiffness of the mechanism must be high enough in order to limit the deflections that can lower the device performance. In Figure 13a and Figure 13c, 300 N forces are applied in the plane XY. This produces an in-plane displacement of less than 20 μm which is small compared to the 0.7 mm that can be generated by the device. In comparison, in Figure 13e, applying 300 N along Z produces a displacement of 10 mm. The in-plane stiffnesses are therefore 200 times greater than along Z. In Figure 13b and Figure 13d, a moment of 100 N.mm around X and Y is applied and produces a rotation of 1.3e-2 rad. In comparison, in Figure 13f applying a moment of 100 N.mm around Z only produces a rotation of 1.0e-5 rad. The torsional stiffness is 1300 times greater than the other rotational stiffnesses.

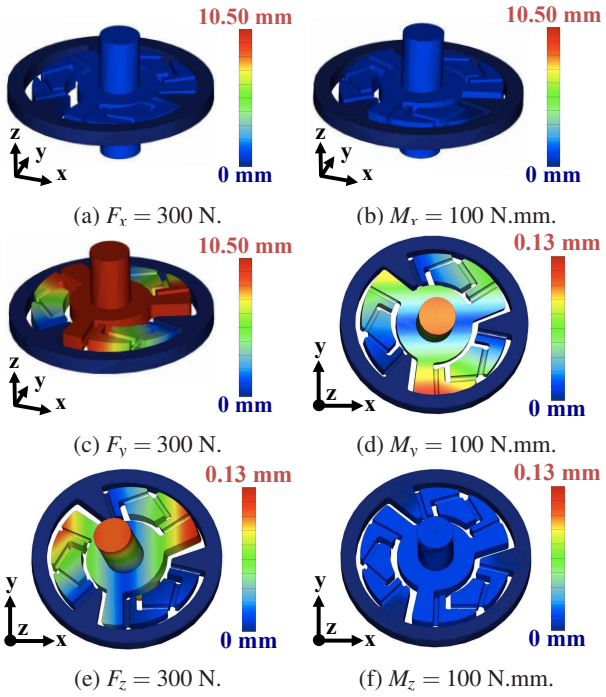

(a) $F_x = 300$ N. (b) $M_x = 100$ N.mm.
(c) $F_y = 300$ N. (d) $M_y = 100$ N.mm.
(e) $F_z = 300$ N. (f) $M_z = 100$ N.mm.

Fig. 13: Finite element analysis of the 3-UU mechanism. Forces F and moments M are applied at the center of the mechanism (color online).

The estimation of the compliance of the 3-UU structure is given by the compliance matrix, a 6×6 matrix, which relates the displacement $\mathbf{u} = [x; y; z; \theta_x; \theta_y; \theta_z]$, in millimeters and in radians, to the load $\mathbf{L} = [F_x; F_y; F_z; M_x; M_y; M_z]$, in newtons and newtons per millimeter, applied at the center of the end-effector:

$$\mathbf{u} = \mathbf{C}.\mathbf{L} \tag{10}$$

The 6×6 compliance matrix $\mathbf{C}$ is evaluated using a finite element analysis (PTC Pro/Mechanica):

$$\mathbf{C} = \begin{bmatrix} \mathbf{4.6e\text{-}5} & 1.0e\text{-}8 & 2.6e\text{-}8 & -4e\text{-}8 & -6.7e\text{-}6 & 3.5e\text{-}9 \\ 5.4e\text{-}8 & \mathbf{4.6e\text{-}5} & 1.6e\text{-}7 & -6.6e\text{-}6 & 8.0e\text{-}6 & 7e\text{-}10 \\ 1.4e\text{-}8 & 2.0e\text{-}8 & \mathbf{3.5e\text{-}2} & 2.3e\text{-}6 & 1.1e\text{-}6 & 2.9e\text{-}9 \\ -5.6e\text{-}9 & 0.0 & 4.6e\text{-}6 & \mathbf{1.3e\text{-}4} & -1.2e\text{-}7 & 9.3e\text{-}11 \\ 0.0 & 1.7e\text{-}9 & 6.8e\text{-}7 & 1.1e\text{-}8 & \mathbf{1.3e\text{-}4} & 2.5e\text{-}9 \\ 1.4e9 & 0.0 & 0.0 & 0.0 & 0.0 & \mathbf{1e\text{-}7} \end{bmatrix} \tag{11}$$

When three forces are applied at the center of the mechanism, there is only a displacement along the vertical axis. When three moments are applied at the center of the mechanism, there are only two significant rotations about in-plane axes. Therefore, from a kinematic point-of-view, the behavior of the mechanism is in accordance with the need for a RRP mechanism.

3.7 Integration into the cardiac stabilizer and new performances

The 3-UU compliant mechanism has been synthesized considering the active stabilizer requirements. The CAD modeling of the whole compensation mechanism composed of the two planes, which integrates the 3-UU compliant mechanism, is illustrated in Figure 14. For the design of the two prismatic joints (Fig. 3), we choose a 2-PRR 1-RR planar mechanism. The 3-UU mechanism is then integrated in the platform of the 2-PRR 1-RR planar mechanism as illustrated in Figure 14a. A first dimensional synthesis of the compliant spherical joint has been performed in [35] according to the requirements for active cardiac stabilization, and is integrated in the device as illustrated in Figure 14b. The planar structures in P_1 and P_2 have thicknesses equal to 5 mm and 6 mm respectively.

Yet, the synthesis has been achieved without an optimization process of the whole device. The presented design allows us to produce a displacement of 0.7 mm which is sufficient to compensate for the flexibilities of the device and the mounting system, according to [12]. With an optimization process, this output displacement could still be increased as the maximal stress level reaches only 82% of the fatigue limit of the material, which is here alloy steel. Finally, the size of the device is divided by four compared to the previous one, the *Cardiolock 2* (Fig. 2). The device compactness is significantly improved by considering an assembly of planar structures.

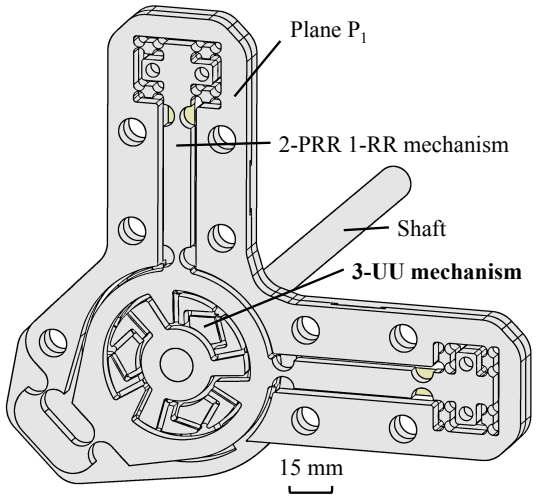

(a) Integration of the 3-UU compliant mechanism into the 2PRR-1RR actuation mechanism.

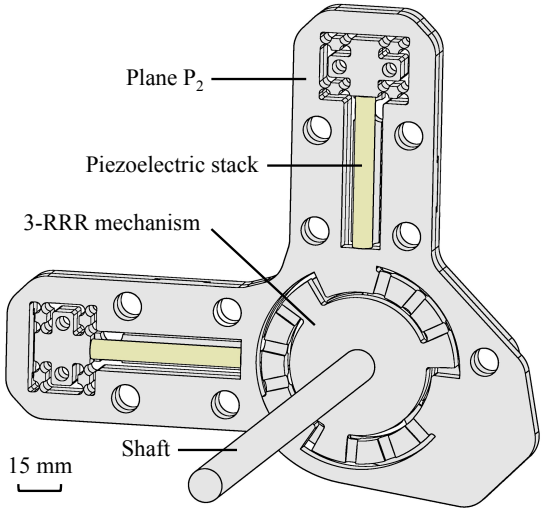

(b) Integration of the compliant 3-RRR orientation mechanism [35].

Fig. 14: CAD view of the final device integrating the different elements composing the compensation mechanism.

4 Conclusion

In this paper a design approach of compliant mechanism based on the analysis of singularities of parallel manipulators has been presented. This approach is an extension of the rigid-body replacement approach that takes advantage of the knowledge of the singularity analysis of parallel manipulators. In addition to taking advantage of the intrinsic stiffness properties of parallel manipulators, the analysis of the singularities in this design approach introduces a simplification step of the compliant mechanism architecture. This design approach has first been presented with the example of the design of 1-DOF compliant mechanism and then successfully applied to the design of a compact 3-DOF compliant mechanism for a surgical device. Finally, an original 3-UU planar compliant mechanism with RRP mobilities has been obtained and presented.

References

[1] Kota, S., Lu, K.-J., Kreiner, Z., Trease, B., Arenas, J., and Geiger, J., 2005. "Design and application of compliant mechanisms for surgical tools". *Journal of Biomechanical Engineering,* ***127***(6), pp. 981–989.

[2] Choi, D., and Riviere, C., 2005. "Flexure-based manipulator for active handhled microsurgical instrument". In 27th Annual International Conference of the IEEE Engineering in Medicine and Biology Society, pp. 2325 – 2328.

[3] Savall, J., Manrique, M., Echeverria, M., and Ares, M., 2006. "Micromanipulator for enhancing surgeon's dexterity in cochlear atraumatic surgery". In IEEE/EMBS Annual International Conference.

[4] Tian, Y., Shirinzadeh, B., and Zhang, D., 2010. "Design and dynamics of a 3-dof flexure-based parallel mechanism for micro/nano manipulation". *Microelectronic Engineering,* ***87***(2), pp. 230 – 241.

[5] Richard, M., and Clavel, R., 2011. "Concept of modular flexure-based mechanisms for ultra-high precision robot design". *Mechanical Sciences,* ***2***(2), pp. 99–107.

[6] Fowler, R. M., Howell, L. L., and Magleby, S. P., 2011. "Compliant space mechanisms: a new frontier for compliant mechanisms". *Mechanical Sciences,* ***2***(2), pp. 205–215.

[7] Gallego, J. A., and Herder, J., 2009. "Synthesis methods in compliant mechanisms: An overview". In ASME 2009 International Design Engineering Technical Conferences and Computers and Information in Engineering Conference, pp. 193–214.

[8] Hopkins, J. B., and Culpepper, M. L., 2011. "Synthesis of precision serial flexure systems using freedom and constraint topologies (fact)". *Precision Engineering,* ***35***(4), pp. 638 – 649.

[9] DiBiasio, C. M., and Culpepper, M. L., 2012. "A building block synthesis approach for precision flexure systems with integrated, strain-based position sensing". *Precision Engineering,* ***36***(4), pp. 673–679.

[10] Olsen, B. M., Issac, Y., Howell, L. L., and Magleby, S. P., 2010. "Utilizing a classification scheme to facilitate rigid-body replacement for compliant mechanism design". In ASME 2010 International Design Engineering Technical Conferences and Computers and Information in Engineering Conference, pp. 475–489.

[11] Howell, L., 2001. *Compliant mechanisms*. Wiley-IEEE.

[12] Bachta, W., Renaud, P., Laroche, E., and Gangloff, J., 2011. "The cardiolock project: Design of an active cardiac stabilizer for cardiac surgery". *ASME Journal of Mechanical Design,* ***133***(7), july, pp. 071002–1–071002–10.

[13] Ouyang, P., 2011. "A spatial hybrid motion compliant mechanism: Design and optimization". *Mechatronics,* ***21***(3), pp. 479 – 489.

[14] Xu, Q., and Li, Y., 2011. "Analytical modeling, optimization and testing of a compound bridge-type compliant displacement amplifier". *Mechanism and Machine Theory,* ***46***(2), pp. 183 – 200.

[15] Olsen, B. M., 2010. "A design framework that employs a classification scheme and library for compliant mechanism design". Master's thesis, Brigham Young University.

[16] Merlet, J.-P., 2006. *Parallel robots*. Springer.

[17] Mattson, C. A., Howell, L. L., and Magleby, S. P., 2004. "Development of commercially viable compliant mechanisms using the pseudo-rigid-body model: Case studies of parallel mechanisms". *Journal of Intelligent Material Systems and Structures,* ***15***(3), March, pp. 195–202.

[18] Amine, S.and Tale-Masouleh, M., Caro, S., Wenger, P., and Gosselin, C., 2012. "Singularity analysis of 3t2r parallel mechanisms using grassmann-cayley algebra and grassmann line geometry". *Mechanism and Machine Theory,* ***52***, pp. 326–340.

[19] Choueifati, J., Lusk, C., Pang, X., and Volinsky, A. A., 2007. "Compliant mems motion characterization by nanoindentation". In MRS Proceedings, Vol. 1052.

[20] Lusk, C. P., and Howell, L. L., 2008. "Components, building blocks, and demonstrations of spherical mechanisms in microelectromechanical systems". *Journal of Mechanical Design,* ***130***(3), p. 034503.

[21] Zlatanov, D., Fenton, R. G., and Benhabib, B., 1995. "A unifying framework for classification and interpretation of mechanism singularities". *Journal of Mechanical Design,* ***117***(4), December, pp. 566–572.

[22] Gosselin, C., and Angeles, J., 1990. "Singularity analysis of closed-loop kinematic chains". *IEEE Transactions on Robotics and Automation,* ***6***, pp. 281–290.

[23] Zlatanov, D. S., 1998. "Classification and interpretation of the singularities of redundant mechanisms". In Proceedings of Design Engineering Technical Conference.

[24] Parise, J. J., Howell, L. L., and Magleby, S. P., 2001. "Ortho-planar linear-motion springs". *Mechanism and Machine Theory,* ***36***(11-12), pp. 1281 – 1299.

[25] Chapuis, D., Gassert, R., Sache, L., Burdet, E., and Bleuler, H., 2004. "Design of a simple mri/fmri compatible force/torque sensor". In IEEE/RSJ International Conference on Intelligent Robots and Systems, Vol. 3, pp. 2593 – 2599 vol.3.

[26] Renaud, P., and de Mathelin, M., 2009. "Kinematic analysis for a novel design of mri-compatible torque sensor". In IEEE/RSJ International Conference on Intelligent Robots and Systems, pp. 2640 –2646.

[27] Bonev, I. A., Zlatanov, D., and Gosselin, C. M., 2003. "Singularity analysis of 3-dof planar parallel mechanisms via screw theory". *Journal of Mechanical Design,* ***125***(3), pp. 573–581.

[28] Lobontiu, N., 2003. *Compliant Mechanisms - design of flexure hinges*. CRC Press.

[29] Trease, B. P., Moon, Y.-M., and Kota, S., 2004. "Design of large-displacement compliant joints". *Journal of Mechanical Design,* ***127***(4), November, pp. 788–798.

[30] Bachta, W., Renaud, P., Laroche, E., Forgione, A., and Gangloff, J., 2008. "Cardiolock: an active cardiac stabilizer, first in vivo experiments using a new robotized device". *Computer Aided Surgery,* ***13***(5), pp. 243–254.

[31] Bachta, W., Renaud, P., Laroche, E., Forgione, A., and Gangloff, J., 2011. "Active stabilization for robotized beating heart surgery". *Robotics, IEEE Transactions on,* ***27***(4), August, pp. 757 –768.

[32] Choi, K.-B., and Lee, H.-W., 2008. "Analysis and design of linear parallel compliant stage for ultra-precision motion based on 4-pp flexural joint mechanism". In International Conference on Smart Manufacturing Application, pp. 35–38.

[33] Wang, H., and Zhang, X., 2008. "Input coupling analysis and optimal design of a 3-dof compliant micro-positioning stage". *Mechanism and Machine Theory,* ***43***(4), pp. 400 – 410.

[34] Yong, Y. K., and Lu, T.-F., 2009. "Kinetostatic modeling of 3-rrr compliant micro-motion stages with flexure hinges". *Mechanism and Machine Theory,* ***44***(6), pp. 1156 – 1175.

[35] Rubbert, L., Renaud, P., and Gangloff, J., 2012. "Design and optimization for a cardiac active stabilizer based on planar parallel compliant mechanism". In Proceedings of the ASME 2012 11th Biennial Conference on Engineering Systems Design and Analysis.

[36] Andersen, C., Magleby, S., and Howell, L., 2009. "Principles and preliminary concepts for compliant mechanically reactive armor". In Proceedings of ASME/IFToMM Int. Conf. on Reconfigurable Mechanisms and Robots, pp. 370 –376.

[37] Qin, Y., and Dai, J. S., 2012. "Forward displacement analysis of two foldable 3us parallel mechanisms". In *Advances in Reconfigurable Mechanisms and Robots I*, J. S. Dai, M. Zoppi, and X. Kong, eds. Springer London, pp. 805–814.

[38] Kong, X., and Gosselin, C., 2007. *Type Synthesis of Parallel Mechanisms*. Springer.

[39] Rubbert, L., Caro, S., Renaud, P., and Gangloff, J., 2012. "A planar rrp compliant mechanism based on the singularity analysis of a 3-us parallel mechanism". In Advances in Robot Kinematics.

[40] Xu, Q., and Li, Y., 2006. "Mechanical design of compliant parallel micromanipulators for nano scale manipulation". In 1st IEEE International Conference on Nano/Micro Engineered and Molecular Systems, pp. 653 –657.

[41] Tanik, E., and Parlaktas, V., 2012. "Compliant cardan universal joint". *Journal of Mechanical Design,* ***134***(2), p. 021011.